國立交通大學

電子工程學系電子研究所

碩士論文

溫度感測探針整合 SU-8 可撓式帶狀纜線於心臟外科手術之應用

Temperature Sensing Probe Integrated with an SU-8 Flexible Ribbon Cable for Heart Surgery Application

研 究 生：李奎樞

指導教授：鄭裕庭　教授

中 華 民 國 九 十 九 年 九 月

溫度感測探針整合 SU-8 可撓式帶狀纜線於心臟外科手術之應用

Temperature Sensing Probe Integrated with an SU-8 Flexible Ribbon Cable for Heart Surgery Application

研 究 生：李奎樞　　Student：Kuei-Shu Li

指導教授：鄭裕庭　　Advisor：Yu-Ting Cheng

國 立 交 通 大 學

電子工程學系電子研究所

碩 士 論 文

A Thesis

Submitted to Department of Electronics Engineering & Institute of Electronics

College of Electrical and Computer Engineering

National Chiao Tung University

in partial Fulfillment of the Requirements

for the Degree of

Master

in

Electronics Engineering

Sep 2010

Hsinchu, Taiwan, Republic of China

中華民國九十九年九月

溫度感測探針整合 SU-8 可撓式帶狀纜線於心臟外科手術之應用

研究生：李奎樞　　指導教授：鄭裕庭　教授

國立交通大學電子工程學系　　電子研究所碩士班

摘　要

本論文呈現磷摻雜之複晶矽電阻式微機械溫度探針整合 SU-8 可撓式軟性纜線之研發製作以期應用於心臟手術之溫度量測。此溫度探針達到 0.9°C 之精準度並可經由準確控制摻雜濃度使得精準度進一步提升。實驗結果顯示探針擁有 4N 之機械強度(套用公式計算)並可在無彎曲折損的情況下輕易刺穿豬心，因此可確認此探針十分適合應用於人體心肌之穿刺定位量測。透過利用先前研發之低溫熱壓式金—金接合技術，SU-8 軟性材料可製作出搭載金屬電性連接導線並且與溫度探針接合建構溫度量測系統以應用於生醫感測之訊號傳輸。可撓式軟性纜線傳輸技術展現生醫元件訊號傳輸之應用性以及微型手術儀器整合之發展潛力。

Temperature Sensing Probe Integrated with an SU-8 Flexible Ribbon Cable for Heart Surgery Application

Student：Kuei-Shu Li Advisor：Dr. Yu-Ting Cheng

Department of Electronics Engineering and Institute of Electronics National Chiao Tung University

Abstract

This thesis presents a p-type boron doped polysilicon resistive based micromachined temperature probe which is integrated with an SU-8/Cu flexible ribbon cable as electrical feedthrough for heart surgery application. The temperature sensor can provide as good as 0.9℃ accuracy and can be further improved by well controlling the doping concentration in the poly-Si for having a larger temperature coefficient of resistance. Experimental results show the probe can easily penetrate pig myocardium with a mechanical strength as strong as 4N which will be good for the temperature measurement in various depths in the myocardium. In addition, combined with a low temperature Au-Au thermal-compressive bond (<200°C), an 82.4cm long flexible cable with 40 metal interconnect lines has been fabricated, bonded, and released from Si wafer to the temperature probe as electrical interconnects for signal transmission from in-situ to outside environment. It's our belief that the flexible feedthrough technology can be applicable to most of the biomedical devices which require transmitting sensed signal to the outside of human body by wire during surgery process.

誌謝

兩年過去了，說長不長說短不短的碩班生活終於到了盡頭。首先感謝的是我的家人，在長久以來的求學生活中總是給我無微不至的照顧，也是我精神上的支柱，希望我的家人們都可以身體健康。謝謝鄭裕庭教授的指導，讓我深刻體會到許多事情不是一蹴可幾，而且常常要比預想的還努力才能達到期望的目標。再來是子元跟阿昌兩位博班學長，惟有你們毫不藏私的傾囊相授，我們在學機台、做實驗時才可以迅速上手，希望你們還有健章學長都可以順利拿到博士學位，也祝健章學長的寶貝女兒平安健康地長大！好同學光頭跟冠名，想當初第一次聊天是在中秋烤肉的時候，兩年來大家一起修課做實驗吃飯打球(閃電手指！)，也在博愛一級戰區培養出革命情感，到了畢業時真的是很不捨，以後一定要多聚聚。松築、震弘、建睿還有 99 級學弟們，祝你們也早日步上軌道，實驗進展順利，準時畢業。還有已經在工作的倫豪學長、退伍倒數的阿富學長跟即將熬出頭的小家學長，祝你們一切順利，有空多回來請客…不是啦，大家約出來吃飯。另外要感謝中央光電所伍茂仁教授、蕭旭良學長跟陳進達同學提供 Flip-Chip Bonder 代工服務讓我可以順利完成研究。最後是交大文服的幾位好朋友，每次跟你們吃喝玩樂總是可以補充正面能量，繼續跟實驗搏鬥。在交大待了六年，熟悉的校園、熟悉的風，收起這段青春歲月結束求學生涯，只希望以後再度踏上這塊土地時，一切都還是如此親切熟稔。交通大學、MIL，再會啦！

Contents

摘　　要 i
Abstract ii
誌謝 iii
Contents iv
Figure Captions v
Table Captions vi
Chapter 1 Introduction 1
Chapter 2 Silicon Probe Design and Fabrication 4
2.1 Probe and Ribbon Cable Design 4
2.2 Probe Section Fabrication Process 7
2.3 SU-8 Flexible Ribbon Fabrication and Bonding Process 9
Chapter 3 Flexible Ribbon Simulation 12
Chapter 4 Temperature Measurement 14
Chapter 5 Conclusion 16
References 17
Vita 19

Figure Captions

Fig. 1-1. Scheme of a silicon probe with temperature sensors and flexible ribbon penetrating into the left ventricular anterior wall. 3

Fig. 2-1. Design of the probe section. The equivalent circuit model is constructed by connecting with a current source and a voltmeter. 4

Fig. 2-2. Illustrations of (a) the probe tip and (b) front view and (c) side view of a simulated shape..... 5

Fig. 2-3. Fabrication process of (a)-(d) silicon probe and (e)-(h) SU-8 ribbon..... 8

Fig. 2-4. Optical photographs of as-fabricated SU-8 flexible ribbon cable. 9

Fig. 2-5. SEM photographs of (a) the probe tip and (b) the Cretan-labyrinth-circular sensor and optical photos of (c) the bonded test chip and (d) a pig's heart with inserted probes. 10

Fig. 2-6. Optical micrographs of the enlarged view on the area of the one end of SU-8 flexible ribbon (a) before and (b) after sacrificial layer removal and optical photographs of (c) test chip in Cr etchant and (d) released device. 11

Fig. 3-1. The simulated and measured z-direction displacements of a 52μm-thick SU-8 spiral structure. The simulated displacement of an 82.4cm-long SU-8 is extrapolated. 13

Fig. 3-2. The scheme of (a) simulated and real extended SU-8 and (b) Von Mises Stress distribution on a 82.4cm long SU-8. 13

Fig. 3-3. The simulated Von Mises stresses near the bonding area under varied extended conditions. 13

Fig. 4-1. Relative resistance variance of the poly-Si sensor before and after bonding. The resistances are measured from about 15°C to 70°C and divided by the resistance at 30°C. The inset is the measured result from 20°C to 40°C. 14

Table Captions

Table 1-1 Comparison of Three Temperature Sensing Technologies 2
Table 4-1 Temperature Measurement Results of Bonded/Unbonded Devices..... 15
Table 5-1 Comparison between Fabricated Sensor/Probe Devices 16

Chapter 1 Introduction

In-vivo probing sensors have been developed for neural signal measurement and stimulation for many years [1], [2]. The probing devices have demonstrated superior biocompatibility and minute tissue damage for biomedical signal measurement and disease therapy. In open heart surgery, the human body is generally under extracorporeal circulation and the heart is kept at a low temperature range from 15 to 30℃ for protecting itself from myocardial necrosis [3], [4]. If the heart temperature rises up, cold blood cardioplegia solution must be perfused into the heart for cooling. Since the heart surface is cooled by a mixture of ice and water during extracorporeal circulation, there must be a temperature gradient formed within myocardium and the temperature inside myocardium would be higher. In general, the esophagus temperature characterized by an esophageal temperature probe is regarded as the heart temperature [5] which cannot be measured directly during the surgery. Thus, the temperature cannot correctly represent the real heart temperature, especially the temperature at the inner part of myocardium, and it could increase the risk of myocardial necrosis. In order to monitor the heart conditions more conscientiously and reduce the risk, a silicon micromachined probe with three circular temperature sensors and a flexible ribbon is designed to detect the temperature at shallow, middle, and deep sites of myocardium respectively.

Three kinds of temperature sensing devices are compared in order to determine a proper technology of temperature sensor (see Table 1-1). Thermocouple is an inexpensive, fast-responsed device but is less accurate and sensitive than the resistance temperature detector (RTD) and the non-linear characteristic is not adequate for short temperature range measurement as previously mentioned application. Thermistor has a good sensitivity and a better accuracy than thermocouple but is fragile due to its ceramic content so it is not applicable to myocardium penetration. RTD is regarded as the best candidate of

temperature sensing technology because it has best accuracy and linearity which are the most required characteristic for short temperature range measurement and the RTD can be fabricated as a micromachined probe by using MEMS process for myocardium penetration detection. Polysilicon is a common structural material in MEMS device fabrication and has a characteristic of linear dependence of resistivity on temperature. The temperature coefficient of resistance (TCR) of p-type doped polysilicon is a constant in the temperature range from room temperature as 25℃ to 150℃ [7]. Therefore, it is a good candidate for the aforementioned application. The TCR is defined as

$$TCR = \frac{1}{R}\frac{\partial R}{\partial T}. \quad (1)$$

For the temperature sensing, we design a Cretan-labyrinth-circular shape with a four-point resistance measurement structure that can provide a better signal to noise ratio. Three temperature sensing structures are then deployed at the designated locations on a micromachined silicon probe which will be inserted in the right or left ventricular anterior wall for fixed-point temperature sensing (see Fig. 1-1).

Table 1-1 Comparison of Three Temperature Sensing Technologies [6]

Criteria	Thermocouple	RTD	Thermistor
Temperature Range	-270℃ to 1800℃	-250℃ to 900℃	-100℃ to 450℃
Accuracy	0.5℃	0.01℃ (platinum) 0.3℃ (poly-Si)	0.1℃
Linearity	Fair	Excellent	Poor
Response Time	Fast	Slow to Medium	Medium
Long Term Stability	Low	High	Medium

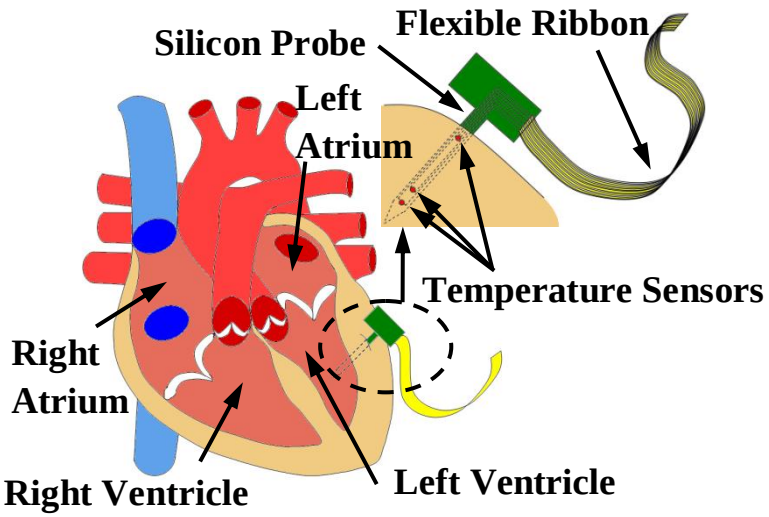

Fig. 1-1. Scheme of a silicon probe with temperature sensors and flexible ribbon penetrating into the left ventricular anterior wall.

So far, most of the biomedical probes are hand-operated in lab, though they have been developed for many years. The connection between the probe and its leads is normally regarded as a critical issue [8], [9] because of the necessity of flexibility for in-situ operation. In this work, SU-8 is chosen as the material for flexible ribbon cable fabrication owing to the superior characteristics of photo-patternable, good chemical stability and biocompatibility, and suitable for fabricating a feature with a high aspect ratio in terms of thickness control…etc. In the work, a ribbon is designed with an 82.4cm-length spiral shape that can provide a proper distance between the probe and the outside measurement instruments and effectively release the stress in the joint while the ribbon is stretched. A wafer-level sacrificial release process will be demonstrated for the flexible ribbon fabrication. By combining the previously developed Au-Au bonding technology [10], the ribbon cable can be electrically connected with the probe for myocardium temperature measurement.

Chapter 2 Silicon Probe Design and Fabrication

2.1 Probe and Ribbon Cable Design

As aforementioned, the probe is needed for various depths sensing, so the shank length is designed as 17mm to place three sensors. The width is as narrow as 300μm in order to avoid a large wound after penetration. By KOH anisotropic etching process, the probe is released from a full wafer with the thickness of 250μm for higher mechanical strength. Fig. 2-1 displays the dimensions of the probe. The distances from three sensors to the cushion pad which ensures the probe can be clamped steadily are 4mm, 12mm and 15mm, respectively. The electrical model is also constructed with one sensor and four leads. The resistance of the sensor can be measured easily by connecting two leads to a current source and the other two to a voltmeter.

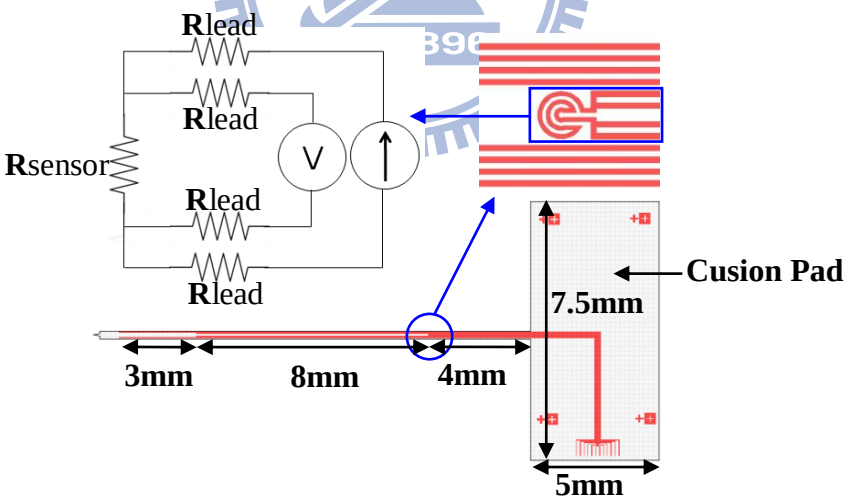

Fig. 2-1. Design of the probe section. The equivalent circuit model is constructed by connecting with a current source and a voltmeter.

To ensure the probe can penetrate into myocardium without bending, the mask is designed as an isosceles triangle with a 100μm base line and a 250μm height as shown in Fig. 2-2 (a). By using IntelliSuite software, the tip shape after KOH anisotropic etching is also simulated and the front view and side view are

shown in Fig. 2-2 (b) (c). The upper and lower lateral angles of the tip are measured as about 45° and 85° while the vertical angle is considerably sharp as about 35°. For an etched <100>-oriented silicon wafer, (111) plane has a lower etch rate than 100 plane and will be exposed after etch. When two (111) planes encounter each other, a comparative blunt lower lateral angle is formed. According to Najafi *et al.* [11], the maximum load (force) P required to buckle a both two ends fixed probe shank is given by

$$P = \frac{EWt^3\pi^2}{6L^2} \tag{2}$$

where E is silicon's elastic modulus (Young's modulus), W is the shank width, t is the thickness, and L is the shank length. Based on the above-mentioned equation, the maximum force is calculated as 4N. Even if the tip becomes blunt and has an area as 1000 μm^2 because of KOH over-etching, it can still provide a pressure as 4GPa which is much larger than the measured Ultimate Strength of bovine myocardium as 0.04MPa [12]. It means that the probe could penetrate myocardium without buckle in the design.

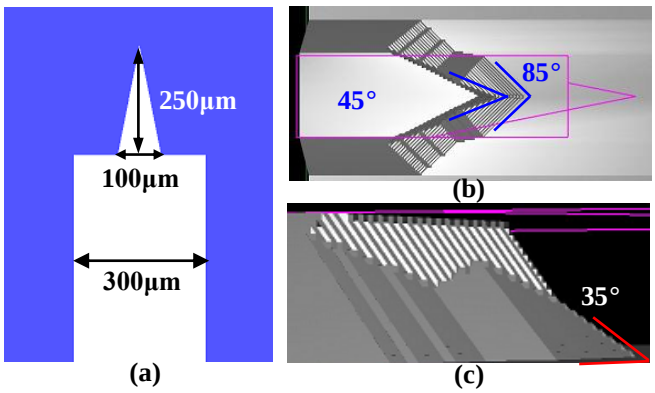

Fig. 2-2. Illustrations of (a) the probe tip and (b) front view and (c) side view of a simulated shape.

The polysilicon film used in this device is deposited using low-pressure chemical vapor deposition (LPCVD) to a thickness of 5000Å and doped with boron of 5×10^{15} cm^{-2} dose to reach low resistance, followed by rapid thermal annealing (RTA) for 1000°C and 30 seconds.

In this work, a SU-8 spiral ribbon structure, whose width, spacing, and total length are designed with 4mm, 4mm, and 82.4cm respectively, are fabricated on a 4" silicon wafer for the demonstration of a long electrical interconnect fabrication between a biomedical device and an interface circuitry system that performs signal processing. In addition, on the ribbon, three distinct metal line structures, whose line width/spacing are designed with 200μm/100μm, 100μm/100μm, and 50μm/50μm respectively, are then fabricated to demonstrate the feasibility for sensor array interconnection.

2.2 Probe Section Fabrication Process

The fabrication process is started with a <100>-oriented silicon wafer of 250μm thickness and standard doping. Fig. 2-3 (a)-(d) shows the process flow of probe fabrication. The wafer is thermal oxidized to a thickness about 3500Å and followed by depositing of 1500Å LPCVD nitride and 2500Å plasma-enhanced chemical vapor deposition (PECVD) TEOS oxide to form an oxide/nitride/oxide stress-balanced dielectric layer structure. Polysilicon is then deposited by LPCVD to 5000Å and doped with boron of 5×10^{15} cm^{-2} dose and then treated by RTA for 1000°C and 30 seconds to get a highly doped and low-resistivity polysilicon film. This poly-Si film is then patterned and etched using Reactive Ion Etching (RIE) to define the sensors, the leads and the bonding pads which are 7μm-in-width, 10μm-in-width and 100μm x 100μm separately. Oxide/Nitride structures are deposited to thickness of 2500Å/1500Å to protect the sensors and the leads. The next process is to pattern the exposed part of the silicon bulk which will be etched by KOH to define the shape of the probe section. The dielectric layers under this pattern are totally etched using RIE and the oxide/nitride layers on the poly-Si pads are also eliminated for the following process. Ti/Cu Seeding layer are sputtered on the full wafer and patterned to expose the bonding pads which are followed by Ni/Au electroless plating to the thickness of 4μm and 0.2μm. A 30% KOH etchant is heated to 70°C to reach a sharp etched shape [13] and the wafer is etched for about five hour to release the probes. The sidewalls of the probes become oblique with an angle of 54.7° due to the distinct etch rates of KOH etchant between (100) plane and (111) plane.

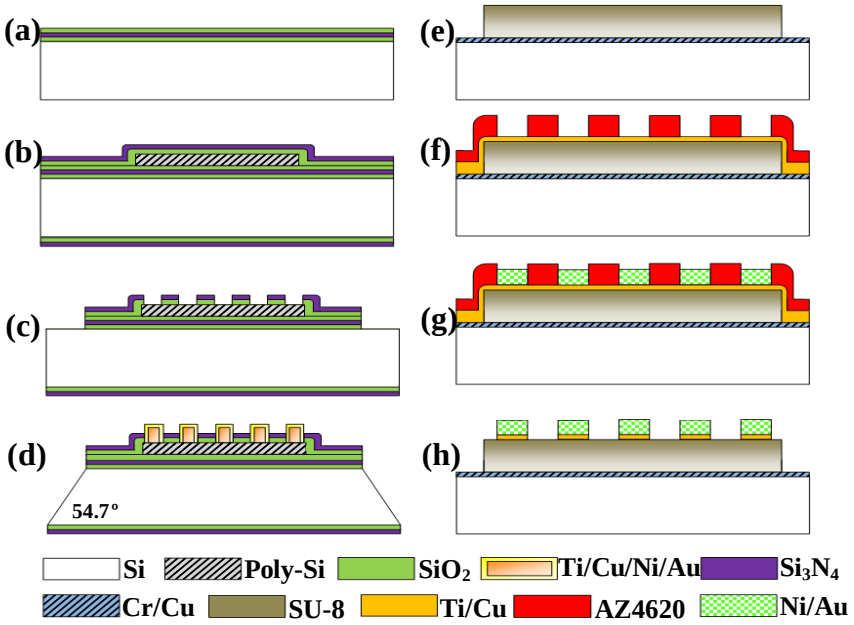

Fig. 2-3. Fabrication process of (a)-(d) silicon probe and (e)-(h) SU-8 ribbon.

2.3 SU-8 Flexible Ribbon Fabrication and Bonding Process

SU-8 is a photo-patternable material, so the shape of the ribbon is constructed by spin-coating and lithography rather than deposition and etching. Fig. 2-3 (e)-(h) depicts the fabrication process flow of the flexible ribbon including: (1) (10nm)Cr/(300nm)Cu sacrificial layer sputter-deposition and 26μm fully cured SU-8 (Gersteltec Sarl GM 2060) spin-coating on a 4" silicon handling wafer, (2) spiral ribbon shaped by lithography and metal line fabrication on the SU-8 by (10nm)Ti/(90nm)Cu seeding layer sputtering and AZ4620 photoresist patterning, followed by Ni/Au electroless plating to the thickness of 4μm and 0.2μm, (3) PR and Ni/Au-uncovered seeding layer removal. Fig. 2-4 shows three kinds of line widths fabricated.

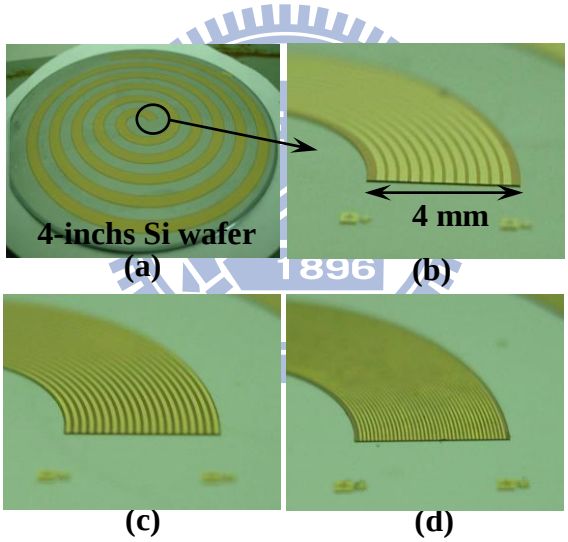

Fig. 2-4. Optical photographs of as-fabricated SU-8 flexible ribbon cable. (a) The SU-8 is patterned as spiral structure for long electrical interconnection. Enlarge view on the one end of SU-8 ribbon, the widths of metal lines are designed with (b) 200μm, (c) 100μm, and (d) 50μm, respectively.

A test chip is also designed for electrical measurement. The chip is 2.8cm long and 1.2cm wide and the SU-8 film is 2.4cm long and 0.4cm wide with 12 metal lines. The chip with ribbons is bonded to a silicon probe by Au-Au thermal compressive bonding technology in 180°C/250°C 2-step bonding for 3min/3min. The bond strength was evaluated as 3.3MPa by shear stress tests in a

JSV-200H test system. The SEM photos of the probe tip and the circular sensor are shown in Fig. 2-5(a) (b) and the optical photos of the bonded test chip and the probe section penetrated into pig's myocardium without any buckle or break are shown in Fig. 2-5(c) (d). The shape of the tip is not very similar to the simulated shape perhaps due to over-etching but it reaches a sharper angle as about 40° and is approached to the simulated upper lateral angle. The handling wafer is detached by etching the Cr/Cu layer and the removal of the sacrificial layer can be clearly observed under an optical microscope due to its transparent characteristic under visible light as shown in Fig. 2-6(a). In addition, the shadow resulted by the bended morphology on the release end of the SU-8 ribbon (see Fig. 2-6(b)) reveals the existence of thermal stress in the SU-8 ribbon. Nevertheless, spiral structure design can effectively release the stress effect which could influence on the device handling. The release process of bonded test chip is also shown in Fig. 2-6(c) (d).

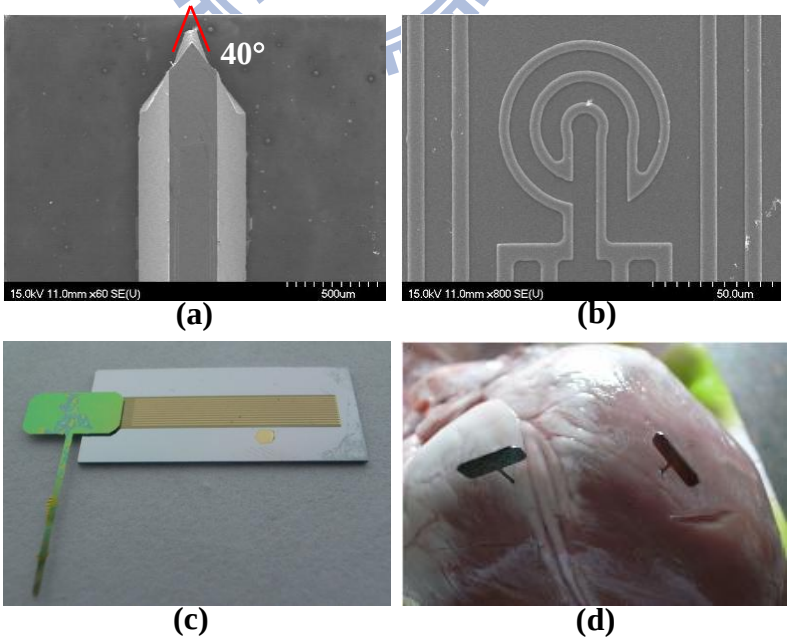

Fig. 2-5. SEM photographs of (a) the probe tip and (b) the Cretan-labyrinth-circular sensor and optical photos of (c) the bonded test chip and (d) a pig's heart with inserted probes.

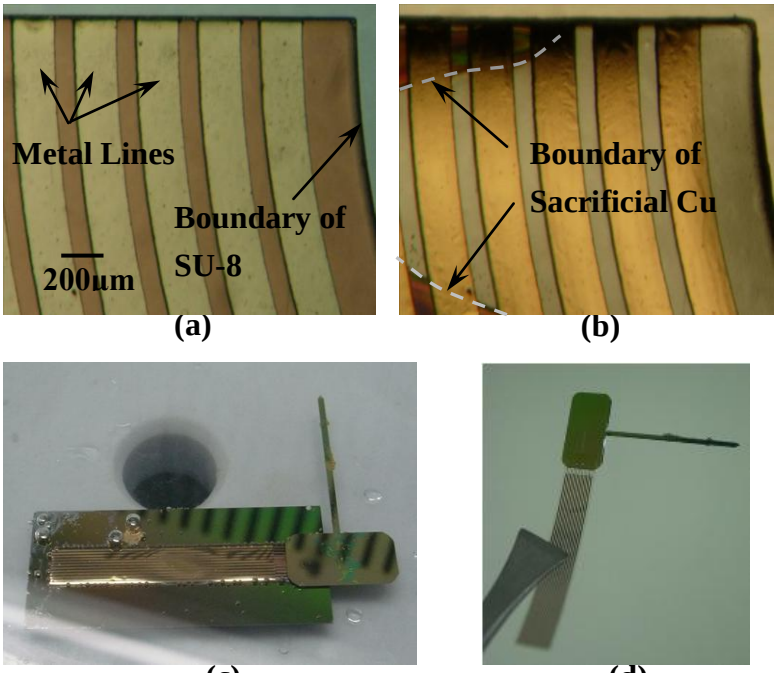

Fig. 2-6. Optical micrographs of the enlarged view on the area of the one end of SU-8 flexible ribbon (a) before and (b) after sacrificial layer removal and optical photographs of (c) test chip in Cr etchant and (d) released device.

Chapter 3 Flexible Ribbon Simulation

For the sake of ensuring the SU-8 flexible ribbon can provide a proper distance between the probe and the measurement instruments, extension simulations are executed using ANSYS software. Fig. 3-1 depicts both the simulated and measured results of the extended displacement in the z-direction of a 52μm-thick SU-8 spiral film which is fixed at one end and naturally hung because of the influence of gravity. The length of SU-8 is simulated from 1.885cm to 21.99cm and the extended distance of a complete 82.4cm-long SU-8 is extrapolated. The two curves are close and the variance between the simulated and measured displacement of an 82.4cm-long spiral ribbon is less than 2.5cm. This result confirmed that the ribbon has a large displacement as 48.5cm under gravity without any pulling force. Fig.3-2 (a) shows the comparison between simulated and real 21.99cm long SU-8 deformed shapes.

The simulated Von Mises stress distribution is shown in Fig. 3-2 (b) and the stresses near the bonding area under extended conditions are shown in Fig. 3-3. Large stresses are distributed on outer circles and the small stresses on inner circles can be observed. The inner end is totally fixed and the outer end is set with 20 to 35cm z-direction displacement. The average stress increases slowly from 39786 Pa to 61142 Pa with the displacement from 20cm to 35cm and the largest Von Mises stress as 0.22MPa is far less than the bond strength mentioned previously as 3.3MPa. These simulation results reveal the SU-8 flexible ribbon cable with metal lines could be extended to 35cm without large stress because the spiral structure could eliminate the stress when the ribbon is stretched.

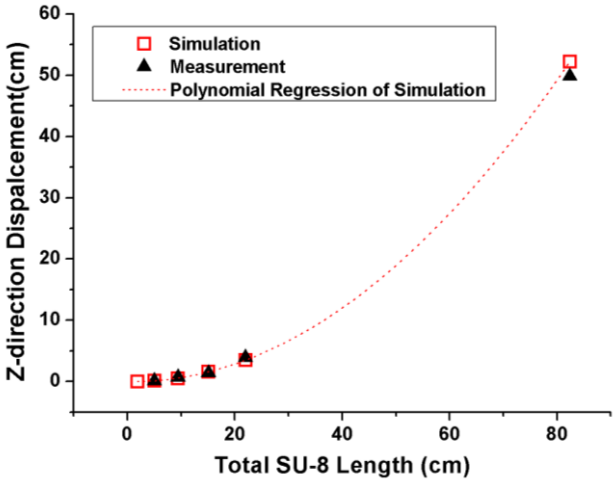

Fig. 3-1. The simulated and measured z-direction displacements of a 52μm-thick SU-8 spiral structure. The simulated displacement of an 82.4cm-long SU-8 is extrapolated.

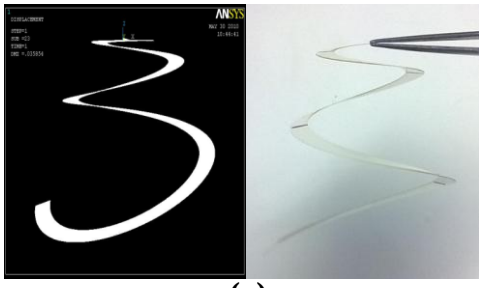

(a)

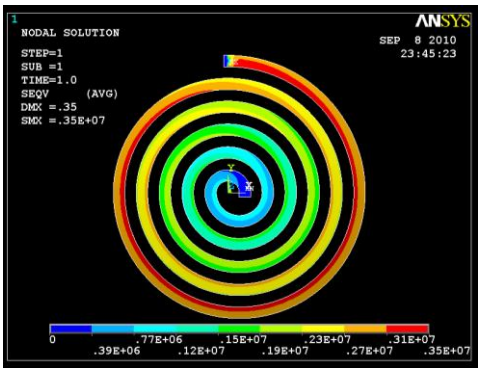

(b)

Fig. 3-2. The scheme of (a) simulated and real extended SU-8 and (b) Von Mises Stress distribution on a 82.4cm long SU-8.

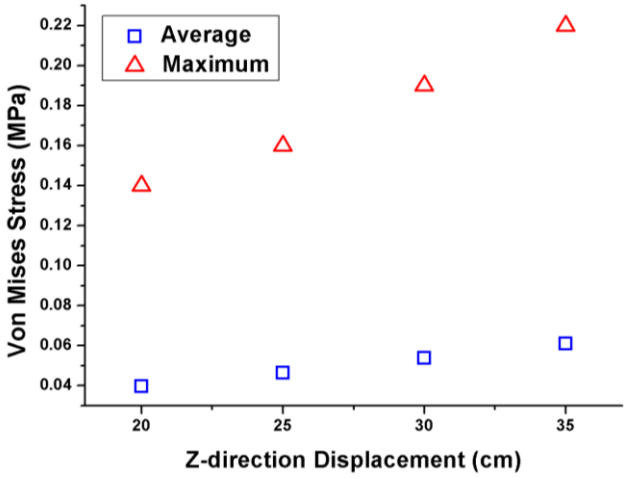

Fig. 3-3. The simulated Von Mises stresses near the bonding area under varied extended conditions.

Chapter 4 Temperature Measurement

The resistance of the temperature sensor in a bonded test chip is measured before and after bonding by a DC current measurement system with Aglient HP 4156B semiconductor parameter analyzer. Owing to the highly doping concentration of the polysilicon, the resistance reaches a contrastive low value and the TCR is negative and approximately linear. Because the TCR is decided by both grain and grain boundary because the grain provides a positive TCR due to impurity scattering and the grain boundary provides a negative TCR due to carrier hopping and diffusion, it would be negative when the temperature dependent characteristic of the grain boundary is dominant [14].

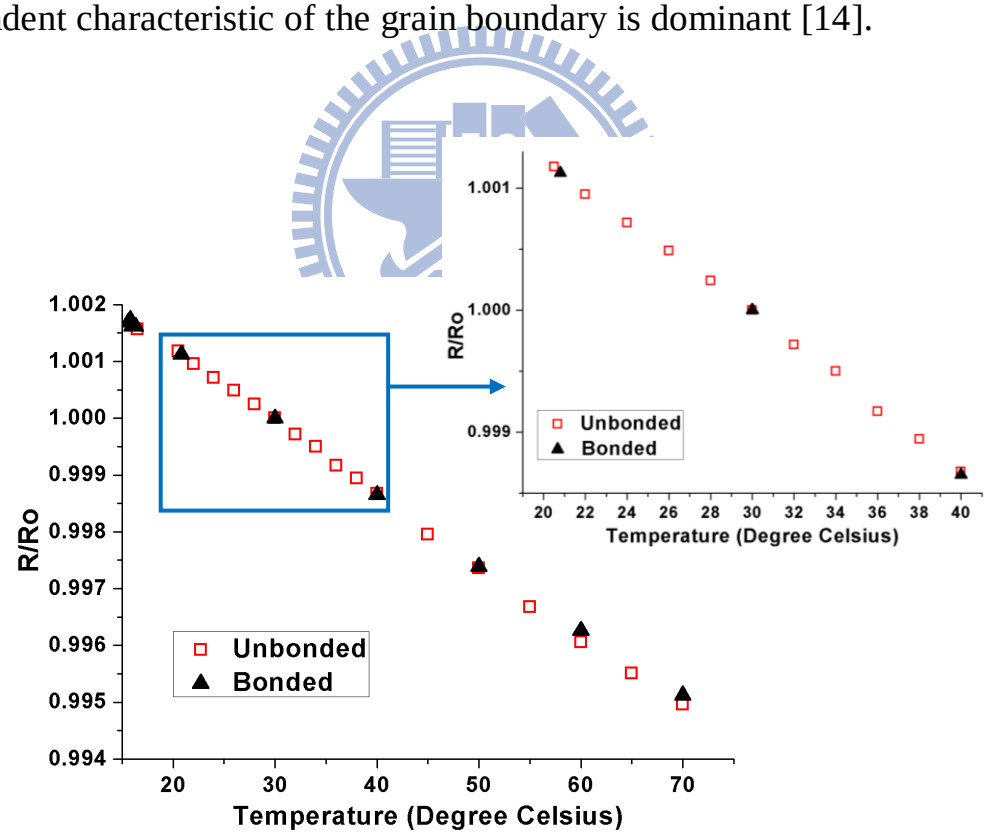

Fig. 4-1. Relative resistance variance of the poly-Si sensor before and after bonding. The resistances are measured from about 15°C to 70°C and divided by the resistance at 30°C. The inset is the measured result from 20°C to 40°C.

The measured range is about 15°C to 70°C and the interval between two

points is 5°C and even 2°C in the important range of 20°C to 40°C. Relative resistance variances of the poly-Si sensor before and after bonding are shown in Fig. 4-1 and the inset of Fig. 4-1 and any wondered point can be extrapolated. The measured resistance is normalized by divided by the resistance at 30°C so that the similarity between the negative linear correlations of temperature and resistance of the before/after bonding devices can be observed more clearly. These two lines are almost overlapped and the TCR variation is less than 5%.

Table 4-1
Temperature Measurement Results of Bonded/Unbonded Devices

	Average TCR (ppm/K)	Linear Regression Equation	Correlation Coefficient	Temperature Accuracy (℃)
Unbonded	-127	y = -0.00256x + 20.2206	-0.99961	+0.8 / -0.7
Bonded	-122	y = -0.0024x + 19.68487	-0.99971	+0.9 / -0.6

Table 4-1 depicts the slopes and the interceptions of the linear regression equations, the TCRs and the correlation coefficients of these two measured datasets. Both two sets of data are nearly negative linear correlated. The temperature accuracy is decided as good as 0.9°C by the largest variance between the measured resistance and the linear regression equation. According to Seto [15] experiments, resistivity depends upon the nature of the dopant and starts to decrease more sufficiently with increasing temperature (more negative TCR) for lower phosphorus and boron concentrations. So, if the doping concentration of the sensor is lower, the accuracy of the temperature microsensors can be upgraded.

Chapter 5 Conclusion

A silicon-based probe with temperature sensors integrated with an SU-8 flexible ribbon is developed for temperature measurement in various depths of myocardium. Table 5-1 shows the comparison between some fabricated sensors or probes [1], [2], [16]. This sensor probe depicts novelties such as direct myocardium temperature sensing, various depths sensor array, large mechanical strength for myocardium penetration and low-stress SU-8 flexible ribbon. The resistance variation is measured and normalized to observe the trend of the TCR. After comparing the measured point and the calculated linear regression line, the accuracy of the temperature sensor is determined as good as 0.9°C in the range of 15°C to 70°C, so the sensor probe is demonstrated to be applicable to temperature sensing for open heart surgery application. The SU-8 flexible ribbon cable reveals the potential of clinical applications like microsurgical tools for electrically connecting the in-situ microdevices to outside instruments.

Table 5-1
Comparison between Fabricated Sensor/Probe Devices

Authors	J. Chen et al. [1]	L. Lin et al. [2]	Z. Bendekovic et al. [16]	This Work
Sensing Mechanism	Polysilicon RTD	N/A	Polysilicon RTD	Polysilicon RTD
Accuracy	0.3°C	N/A	5% (Worst Accuracy)	0.9°C
Shank Dimensions	2mm(l) 60μm(w) 15μm(t)	1-6mm(l) 80-140μm(w) 70μm(t)	N/A	17mm(l) 300μm(w) 250μm(t)
Mechanical Strength	0.012N	0.33N	N/A	4N
Device Application	Neural Tissue Thermal Marking	Microchannel	Temperature Measurement (200-800K)	Myocardium Temperature Sensing

References

[1] J. Chen and K. D. Wise, "A Silicon Probe with Integrated Microheaters for Thermal Marking and Monitoring of Neural Tissue" *IEEE Trans Biome Eng*, vol. 44, pp. 770-774, 1997.

[2] L. Lin and A. P. Pisano "Silicon-Processed Microneedles" *IEEE JMEMS*, vol. 8, pp.78-84, 1999.

[3] W. C. Sealy, I. W. Brown, JR., W. G. Young, JR. "A Report on the Use of Both Extracorporeal Circulation and Hypothermia for Open Heart Surgery" *Annals of Surgery*, vol. 147, pp.603-613, 1958.

[4] W. C. Sealy, I. W. Brown, JR., W. G. Young, W. W. Smith, A. M. Lesage "Hypothermia and Extracorporeal Circulation for Open Heart Surgery: Its Simplification with a Heat Exchanger for Rapid Cooling and Rewarming" *Annals of Surgery*, vol. 150, pp.627-639, 1959.

[5] R. H. Patterson, JR., B. S. Ray "Profound Hypothermia for Intracranial Surgery: Laboratory and Clinical Experiences with Extracorporeal Circulation by Peripheral Cannulation" *Annals of Surgery*, vol. 156, pp.377-393, 1962.

[6] B.C. Baker, "Temperature sensing technologies", AN 679 microchip Inc., pp.1-9, 1998.

[7] H. Chuang, K. Thei, S. Tsai, and W. Liu "Temperature-Dependent Characteristics of Polysilicon and Diffused Resistors" *IEEE TED*, vol. 50, pp.1413-1415, 2003.

[8] S. Kisban, T. Holzhammer, S. Herwik, O. Paul and P. Ruther "Novel Method for the Assembly and Electrical Contacting of Out-of-Plane Microstructures" *IEEE MEMS Conf*, pp.484-487, 2010.

[9] S. Chuang, C. Chen, H. Su, S. Yeh, and D. Yao "Design and Fabrication of Flexible Neural Microprobe for Three Dimensional Assembly" *IEEE MEMS Conf*, pp.1003-1006, 2010.

[10] T.-Y. Chao, C.-H. Li, Y. C. Chen, H.-Y. Chen, Y. T. Cheng, and C.-N. Kuo "An Interconnecting Technology for RF MEMS Heterogeneous Chip Integration" accepted by *IEEE TED*.

[11] K. Najafi, J. F. Hetke "Strength Characterization of Silicon Microprobes in Neurophysiological Tissues" *IEEE Trans Biome Eng*, vol. 37, pp.474-481, 1990.

[12] J.T. Walsh Jr, T.F. Deutsch "Pulsed CO2 laser ablation of tissue: effect of mechanical properties" *IEEE Trans Biome Eng*, vol. 36, pp.1195-1201, 1989.

[13]M. H. Yun, V. A. Burrows, and M. N. Kozicki “Analysis of KOH etching of .100. silicon on insulator for the fabrication of nanoscale tips” *J. Vac. Sci. Technol. B*, vol. 16, pp.2844-2848, 1998.
[14]M. S. Raman, T. Kifle, E. Bhattacharya, and K. N. Bhat “Physical Model for the Resistivity and Temperature Coefficient of Resistivity in Heavily Doped Polysilicon” *IEEE TED*, vol. 53, pp.1885-1892, 2006.
[15]J. Y. W. Seto “The electrical properties of polycrystalline silicon films” *Journal of Applied Physics*, vol. 46, pp.5247-5254, 1975.
[16]Z. Bendekovic, P. Biljanovic D. Grgec “POLYSILICON TEMPERATURE SENSOR” *IEEE MELECON*, pp.362-365, 1998.

Vita

姓名：李奎樞

性別：男

生日：民國七十五年四月九日

籍貫：台灣新竹

地址：新竹縣竹北市中央路 229 號 6 樓

學歷：國立交通大學電子工程學系

（93 年 9 月~97 年 6 月）

國立交通大學電機學院電子工程研究所碩士班

（97 年 9 月~99 年 9 月）

論文題目：

溫度感測探針整合 SU-8 可撓式帶狀纜線於心臟外科手術之應用

Temperature Sensing Probe Integrated with an SU-8 Flexible Ribbon Cable for Heart Surgery Application